

# Sliding Mode Control with Sliding Perturbation Observer for Surgical Robots

Young-Eun Song<sup>1</sup> Chi-Yen Kim<sup>2</sup> Min-Cheol Lee<sup>3</sup>

<sup>1</sup> Department of Mechanical Engineering, Pusan National University, Busan, Korea  
(Tel : +82-51-510-3081; E-mail: tdsong@pusan.ac.kr)

<sup>2</sup> Department of Mechanical Engineering, Pusan National University, Busan, Korea  
(Tel : +82-51-510-3081; E-mail: chiykim@pusan.ac.kr)

<sup>3</sup> Department of Mechanical Engineering, Pusan National University, Busan, Korea  
(Tel : +81-51-510-2439; E-mail: mcllee@pusan.ac.kr)

**Abstract**-Minimally invasive surgery (MIS) robot is made like a long cylinder with small diameter that can fit through a small incision thus decreasing the amount of healthy tissue damaged. Because of the shape of the surgical robot, the cable-driven mechanism is using to the robot. However this is a highly nonlinear system so the performance of the system is not so good. This paper applied a robust motion control algorithm. The algorithm uses partial state feedback for a class of nonlinear systems with modeling uncertainties and external disturbances. The major contribution is the design of a robust observer for the state and the perturbation of the instrument of the surgical robot, which is combined with a variable structure controller (VSC). The combination of controller and observer provides the robust routine called sliding mode control with sliding perturbation observer (SMCSPO). The control performance of the proposed algorithm is evaluated by the simulation and experiment to apply to a two-degree-of-freedom (DOF) robot arm. The results showed high accuracy and good performance.

## I. INTRODUCTION

Robotic-assisted surgery is an emerging field because of the benefits in dexterity and tremor reduction that the robots can provide. In recent years the prevalence of the robotic-assisted surgery systems in medical systems has increased. Especially, because of the ability of robotic manipulators to make small, precise movements, robotic systems are a good match for MIS [1]. However to achieve small size of the robotic tool tip, cables drive the force of motors, similar to human tendons, such as EndoWrist Instrument as shown in Fig. 1. This cable-driven mechanism is a highly nonlinear system due to the tension of a cable and complex structure. So the control performance of the robotic surgeon system is not so good. It thus appears that the nonlinearity measurement of the system is really desirable due to ensure the precision control.

The major contribution of the design of robust controller for the surgical robot introduces the development and design of

robust observer for the state and the perturbation, which is integrated into a variable structure controller structure [2], [3].

The combination of controller and observer gives rise to the robust routine called SMCSPO. Sliding observer (SO) is a high performance state estimator well suited for nonlinear uncertain systems with partial state feedback [4]. Therefore, system doesn't need additional sensor.

The sliding function of this observer consists of the estimation error of the available output. The SO does not require a full state feedback in the perturbation estimation and reduces the implementation costs [3].

The combined observer, which is able to provide much better accuracy of state estimate, called sliding perturbation observer (SPO) [5]. The combination of this SPO and sliding mode controller (SMC) results in a high performance algorithm that is robust against perturbations, utilizes only partial state feedback. Furthermore, we introduce the robust control gain to remove the restrictions of SMC and SPO.

In this paper, ahead of applying to the instrument of a surgical robot, this robust motion control algorithm using partial state feedback for a class of nonlinear systems with modeling uncertainties and external disturbances is previously applied to a 2 DOF robot arm to evaluate the control performance. Also, the optimal gains of the motion control algorithm are easily obtained by eigenvalue composition.



Fig. 1. EndoWrist Instrument

This paper is organized as follows: In Section 2, design of SPO is introduced. In Section 3, composition of controller and algorithm for selecting robust control gain is designed. In Section 4, the designed approach is evaluated through simulation and experiment. This paper concludes in Section 5.

## II. DESIGN OF SLIDING PERTURBATION OBSERVER

This section describes the applied perturbation observer without considering the closed-loop control. The developed robotic instrument test kit is shown as Fig. 2.

### A. Definition of Perturbation

Generally, the governing equation of a class of nonlinear system is defined as

$$\mathbf{x}^{(n)} = \mathbf{f}(\mathbf{X}_1, \dots, \mathbf{X}_m) + \Delta\mathbf{f}(\mathbf{X}_1, \dots, \mathbf{X}_m) + (\mathbf{B}(\mathbf{X}_1, \dots, \mathbf{X}_m) + \Delta\mathbf{B}(\mathbf{X}_1, \dots, \mathbf{X}_m))\mathbf{u} + \mathbf{d}(t) \quad (1)$$

where

$\mathbf{X}_i \equiv [\mathbf{x}_i, \dot{\mathbf{x}}_i, \dots, \mathbf{x}_i^{(n_i-1)}]^T \in \mathbb{R}^{n_i}$ ,  $i=1, \dots, m$  : the state sub-vector, which forms the global state vector

$[\mathbf{X}_1^T, \dots, \mathbf{X}_m^T]^T \in \mathbb{R}^r$ ,  $r = \sum_{i=1}^m n_i$ ,  $i=1, \dots, m$  : independent coordinate

$\mathbf{f} = [f_1, \dots, f_m]^T \in \mathbb{R}^m$  and  $\Delta\mathbf{f} = [\Delta f_1, \dots, \Delta f_m]^T \in \mathbb{R}^m$  : vector fields corresponding to the uncertainties of nonlinear driving terms and their perturbations, respectively

$\mathbf{B} = [b_{ij}] \in \mathbb{R}^{m \times m}$  and  $\Delta\mathbf{B} = [\Delta b_{ij}] \in \mathbb{R}^{m \times m}$ ,  $i, j = 1, \dots, m$  : matrices representing control gains and their uncertainties

$\mathbf{d} = [d_1, \dots, d_m]^T \in \mathbb{R}^m$  : disturbance vector of the system

$\mathbf{u} = [u_1, \dots, u_m]^T \in \mathbb{R}^m$  : control vector

$\mathbf{x}^{(n)} = [x_1^{(n)}, \dots, x_m^{(n)}]^T \in \mathbb{R}^m$ ,  $x_i^{(n)} \in \mathbb{R}$  with

$$x_i^{(k)} = \frac{d^k(x_i)}{dt^k}, \dot{x}_i = \frac{d(x_i)}{dt}$$

The perturbations  $\Delta\mathbf{f}$ ,  $\Delta\mathbf{B}$ ,  $\mathbf{d}$  are not known but assumed to be bounded by a known continuous functions of  $\mathbf{X}_i$ ,  $i=1, \dots, m$  and  $t$  [4]

In the governing equation, perturbation is defined as the combination of all the uncertainties and nonlinear term of (1).

$$\Psi(\mathbf{X}_1, \dots, \mathbf{X}_m, t) = \Delta\mathbf{f}(\mathbf{X}_1, \dots, \mathbf{X}_m) + \Delta\mathbf{B}(\mathbf{X}_1, \dots, \mathbf{X}_m)\mathbf{u} + \mathbf{d}(t) \quad (2)$$

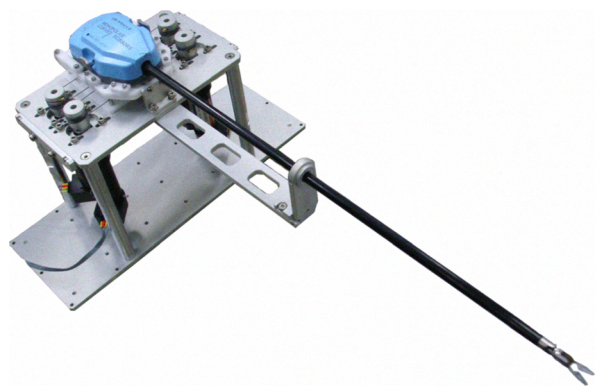


Fig. 2. Robotic instrument test kit

The control task is to derive the state sub-vector toward a desired state vector  $\mathbf{X}_{id} = [x_{id}, \dot{x}_{id}, \dots, x_{id}^{(n_i-1)}]^T$  despite these perturbations [4]. It is assumed that the perturbations are upper bounded by a known continuous function of the state such as

$$\Gamma(\mathbf{X}_1, \dots, \mathbf{X}_m, t) = F(\mathbf{X}_1, \dots, \mathbf{X}_m) + |\Phi_{ji}(\mathbf{X}_1, \dots, \mathbf{X}_m)\mathbf{u}| + D(t) > |\Psi(t)| \quad (3)$$

where  $F > |\Delta\mathbf{f}|$ ,  $\Phi > |\Delta\mathbf{B}|$ ,  $D > |\mathbf{d}|$  represent the expected upper bounds of the uncertainties, respectively.

### B. Sliding Perturbation Observer

The new control variable that is used in order to decouple the control of (1) is defined as

$$\mathbf{f}(\hat{\mathbf{X}}_1, \dots, \hat{\mathbf{X}}_m) + \Delta\mathbf{B}(\hat{\mathbf{X}}_1, \dots, \hat{\mathbf{X}}_m)\mathbf{u} = \alpha_{3j}\bar{u}_j \quad (4)$$

where  $x$  is the state,  $\alpha_{3j}$  is an arbitrary positive number and  $\bar{u}_j$  is the new control variable [5], [6]. Throughout the text, “~” and “^” symbolize the estimation errors and quantity respectively.

The state representation of the simplified dynamics is like (5)

$$\dot{x}_{1j} = x_{2j} \quad (5a)$$

$$\dot{x}_{2j} = \alpha_{3j}\bar{u}_j + \Psi_j \quad (5b)$$

$$y_j = x_{1j} \quad (5c)$$

where "j" is the number of robot arm joint number.

Let  $x_{3j}$  be a new state variable which defined as (6).

$$x_{3j} = \alpha_{3j}x_{2j} - \Psi_j / \alpha_{3j} \quad (6)$$

It is desirable to observe the variable and to consequently calculate  $\Psi_j$  instead of estimating them directly. In order to accomplish this, it is assumed that the perturbations are continuous and lie within a known finite frequency range [6].

The estimated perturbation  $\hat{\Psi}_j$  needs the estimated state,  $x_{2j}$ . The sliding perturbation observer is better than the general one because this observer can provide an on-line perturbation estimation scheme using only partial state feedback. Also, the estimation accuracy of  $x_{2j}$  improves the accuracy of the perturbation estimation. This structure [3] can be achieved by writing the observer equation as

$$\dot{\hat{x}}_{1j} = \hat{x}_{2j} - k_{1j} \text{sat}(\tilde{x}_{1j}) - \alpha_{1j} \tilde{x}_{1j} \quad (7a)$$

$$\dot{\hat{x}}_{2j} = \alpha_{3j} \bar{u}_j - k_{2j} \text{sat}(\tilde{x}_{1j}) - \alpha_{2j} \tilde{x}_{1j} + \hat{\Psi}_j \quad (7b)$$

$$\dot{\hat{x}}_{3j} = \alpha_{3j}^2 (-\hat{x}_{3j} + \alpha_{3j} \hat{x}_{2j} + \bar{u}_j) \quad (7c)$$

where  $\hat{\Psi}_j$  is derived as

$$\hat{\Psi}_j = \alpha_{3j} (-\hat{x}_{3j} + \alpha_{3j} \hat{x}_{2j}) \quad (8)$$

$$k_{1j}, k_{2j}, \alpha_{1j}, \alpha_{2j} > 0$$

$\tilde{x}_{1j} = \hat{x}_{1j} - x_{1j}$  is the estimation error of the measurable state, and  $\text{sat}(\tilde{x}_{1j})$  is the saturation function for the existence of sliding mode.

### III. COMPOSITION OF CONTROLLER AND GAIN OPTIMIZATION OF SMCSPO

#### A. Design Procedure

The estimated sliding function define as

$$\hat{s}_j = \dot{\hat{e}}_j + c_{j1} \hat{e}_j \quad (9)$$

where  $c_{j1} (> 0)$  is a slope of switching line and  $\hat{e}_j (= \hat{x}_{1j} - x_{1dj})$  is the estimated position tracking error.  $[x_{1dj} \ \dot{x}_{1dj}]^T$  is the desired states for the motion of the robot arm. The control  $\bar{u}_j$  is selected to enforce  $\hat{s}_j^T \hat{s}_j < 0$  outside a prescribed manifold. A desired  $\hat{s}_j$  is like as

$$\dot{\hat{s}}_j = -K_j \text{sat}(\hat{s}_j) \quad (10)$$

where

$$\text{sat}(\hat{s}_j) = \begin{cases} \hat{s}_j / |\hat{s}_j|, & \text{if } |\hat{s}_j| \geq \varepsilon_{sj} \\ \hat{s}_j / \varepsilon_{sj}, & \text{if } |\hat{s}_j| \leq \varepsilon_{sj} \end{cases} \quad (11)$$

is used due to its desirable anti-chatter properties and  $K_j (> 0)$  is the robust control gain. In this equation,  $\varepsilon_{sj}$  depicts the width of boundary layer of the SMC, which is different value with the boundary layer  $\varepsilon_{oj}$  in SPO [8].

Using (7), (8), (9), (10), and (11) it is possible to compute  $\dot{\hat{s}}_j$  as

$$\begin{aligned} \dot{\hat{s}}_j = & \alpha_{3j} \bar{u}_j - [k_{2j} / \varepsilon_{oj} + c_{j1} (k_{1j} / \varepsilon_{oj}) - (k_{1j} / \varepsilon_{oj})^2] \tilde{x}_{1j} \\ & + \ddot{x}_{1dj} + c_{j1} (\hat{x}_{2j} - \dot{x}_{1dj}) + \beta_j \hat{\Psi}_j \end{aligned} \quad (12)$$

The resulting  $|\hat{s}_j|$ -dynamics including the effects of  $\tilde{x}_{2j}$  is selected as

$$\dot{\hat{s}}_j = -K_j \text{sat}(\hat{s}_j) - (k_{1j} / \varepsilon_{oj}) \tilde{x}_{2j} - K_{Sj} \hat{s}_j - K_{Rj} \sigma_j \quad (13)$$

where  $K_{Sj} (> 0)$  is the recursive filter gain and  $K_{Rj} (> 0)$  is the robust control gain to remove the restrictions of SMC and SPO. In order to enforce (6) when  $\tilde{x}_{2j} = 0$ , a control law is selected as

$$\begin{aligned} \bar{u}_j = & \frac{1}{\alpha_{3j}} \{ -K_j \text{sat}(\hat{s}_j) - (k_{1j} / \varepsilon_{oj}) \tilde{x}_{2j} \\ & + [k_{2j} / \varepsilon_{oj} + c_{j1} (k_{1j} / \varepsilon_{oj}) - (k_{1j} / \varepsilon_{oj})^2] \tilde{x}_{1j} + \ddot{x}_{1dj} \\ & - c_{j1} (\hat{x}_{2j} - \dot{x}_{1dj}) - K_{Sj} \hat{s}_j - K_{Rj} \sigma_j - \beta_j \hat{\Psi}_j \} \end{aligned} \quad (14)$$

where  $\beta_j$  is positive gain of perturbation and  $\beta_j \hat{\Psi}_j$  is upper bounded by a known continuous function of the state such as (3).

The conditions for the existence of sliding mode are given by

$$\text{sat}(\tilde{x}_{1j}) = \begin{cases} \tilde{x}_{1j} / |\tilde{x}_{1j}|, & \text{if } |\tilde{x}_{1j}| \geq \varepsilon_{oj} \\ \tilde{x}_{1j} / \varepsilon_{oj}, & \text{if } |\tilde{x}_{1j}| \leq \varepsilon_{oj} \end{cases} \quad (15)$$

The observer's sliding mode takes place on the line  $\tilde{x}_{1j} = 0$  of the observer state space  $\tilde{x}_{1j}$  vs.  $\tilde{x}_{2j}$ . The conditions for the existence of sliding mode are

$$\tilde{x}_{2j} \leq \alpha_{1j} \tilde{x}_{1j} + k_{1j} \quad (\text{if } \tilde{x}_{1j} > 0) \quad (16a)$$

$$\tilde{x}_{2j} \geq \alpha_{1j} \tilde{x}_{1j} - k_{1j} \quad (\text{if } \tilde{x}_{1j} < 0) \quad (16b)$$

From the sliding condition (10), the state estimation error is bounded by  $|\tilde{x}_{2j}| \leq k_{1j}$ . Therefore, in order to satisfy  $\hat{s}_j^T \hat{s}_j < 0$  outside the manifold  $|\hat{s}_j| \leq \varepsilon_{oj}$ , the robust control gains must be chosen such as

$$\begin{aligned} K_j &\geq (\Delta \mathbf{f} + \Delta \mathbf{B} \mathbf{u} + \mathbf{d})_{j, \text{worst case}} \\ K_{Rj} &\geq K_{Sj} \geq K_j \geq k_{1j}^2 / \varepsilon_{oj} \end{aligned} \quad (17)$$

A systematic general design procedure considering the hardware limitations of the system is described by the fact that the eigenvalues of the characteristic equation of systematic matrix of observer and  $s_j$  dynamics are negative real number. For simplicity, all the desired poles are selected to be the same real valued location  $\lambda = -\lambda_d$  ( $\lambda_d > 0$ ). This leads to the following design solution.

$$\begin{aligned} \frac{k_{1j}}{\varepsilon_{oj}} &= 3\lambda_d, \quad \frac{k_{2j}}{k_{1j}} = \lambda_d, \\ \alpha_{3j} &= \sqrt{\frac{\lambda_d}{3}}, \quad c_{j1} = K_j / \varepsilon_{oj} = \lambda_d \end{aligned} \quad (18)$$

Physical limitations of the control system define the optimum placement of  $\lambda_d$ . The  $\lambda_d$  is effected by hardware constraints such as sampling frequency, dominant time delay, measurement delay and actuator dynamics [5],[6].

#### IV. SIMULATION AND EXPERIMENT

##### A. Simulation

This section shows simulation results applying to the 2 DOF robot arm as shown in Fig. 3, which has nonlinear terms so as to evaluate the control performance.

$$\begin{bmatrix} \ddot{\theta}_1 \\ \ddot{\theta}_2 \end{bmatrix} = \begin{bmatrix} f_1 \\ f_2 \end{bmatrix} + \begin{bmatrix} g_{11} & g_{12} \\ g_{21} & g_{22} \end{bmatrix} \begin{bmatrix} u_1 \\ u_2 \end{bmatrix} + \begin{bmatrix} d_1 \\ d_2 \end{bmatrix} \quad (19)$$

where

$$\begin{aligned} g_{11} &= \frac{1}{a_1^2(m_1 + m_2 - m_2 \cos^2 \theta_2)} \\ g_{12} = g_{21} &= \frac{-a_2 - a_1 \cos \theta_2}{a_1^2 a_2 (m_1 + m_2 - m_2 \cos^2 \theta_2)} \\ g_{22} &= \frac{a_2^2 m_2 + a_1^2 (m_1 + m_2) + a_1 a_2 m_2 \cos \theta_2}{a_1^2 a_2^2 m_2 (m_1 + m_2 - m_2 \cos^2 \theta_2)} \end{aligned}$$

$$f_1 = -g_{11} m_2 a_1 a_2 (2\dot{\theta}_1 \dot{\theta}_2 + \dot{\theta}_2^2) \sin \theta_2 + g_{12} m_2 a_1 a_2 \dot{\theta}_1^2 \sin \theta_2$$

$$f_2 = -g_{21} m_2 a_1 a_2 (2\dot{\theta}_1 \dot{\theta}_2 + \dot{\theta}_2^2) \sin \theta_2 + g_{22} m_2 a_1 a_2 \dot{\theta}_1^2 \sin \theta_2$$

$u_i$  ( $i=1,2$ ) is the control torque. The numerical parameters are:  $l_1 = l_2 = 1.0m$ ;  $m_1 = m_2 = 5.0Kg$ . The command trajectories for tracking are given by  $\theta_{1d} = 30 \sin(2\pi t / 5)$  and  $\theta_{2d} = 50 \sin(1\pi t / 5)$  respectively.

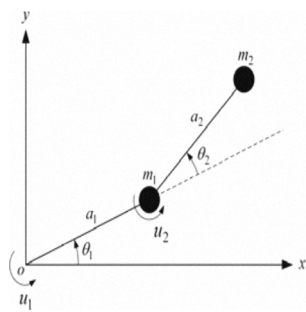


Fig. 3. 2 DOF robot arm

The control loop is closed at 100 Hz sampling rate. It is assumed that the sampling period is dominant time delay of the closed loop system. Table 1 shows the parameter for simulation. The parameter was selected by trial and error.

In the result of simulation, it is shown that the SO performance is so good as shown in Fig. 4.

Also, the magnitude of the calculated nonlinear term is similar to the estimated perturbation term as shown in Fig. 5.

##### B. Experimental Results

In order to evaluate the proposed control algorithm, SMC is compared with SMCSPO. The control input of SMC is given by

$$u_j = I \left[ -K_j \text{sat}(s_j) - c_j \dot{e} + \ddot{\theta}_{jd} \right] \quad (20)$$

where  $K_j = \text{diag}[K_j]$  ( $K_j > 0$ ),  $\dot{e}_j = [\dot{e}_1 \dots \dot{e}_4]^T$ ,  $\text{sat}(s_j) = [\text{sat}(s_1) \dots \text{sat}(s_4)]^T$ , and  $\ddot{\theta}_{jd} = [\ddot{\theta}_{1d} \dots \ddot{\theta}_{4d}]^T$ .

The control gains are chosen as  $K_j = 20.43$  and  $c_j = 20.43$ . The 2 DOF robot is used in experiment which is shown as Fig. 6.

TABLE I  
PARAMETER SELECTIONS OF SIMULATION

Parameter	Value
$k_{1i} / \varepsilon_{oi}$	20
$k_{2i} / K_{1i}$	48
$\alpha_{3i}$	5.2
$K_i$	38
$K_{S_i}$	51
$K_{R_i}$	112

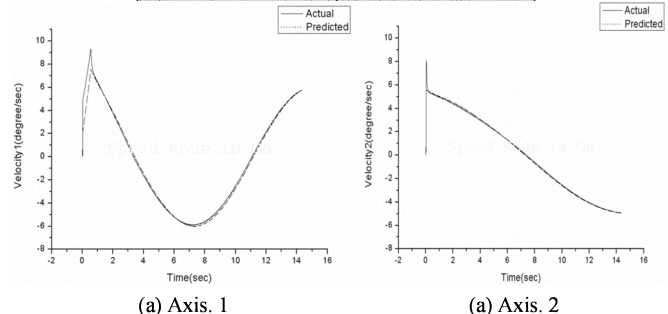


Fig. 4. Velocity estimate results

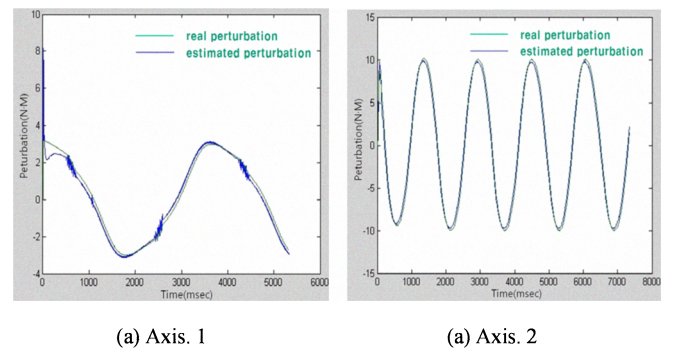


Fig. 5. Perturbation estimate results

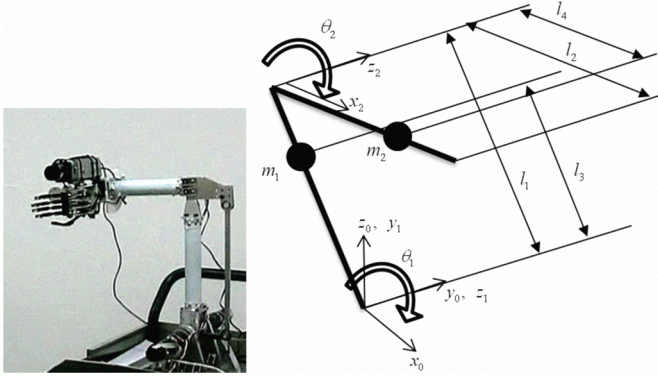


Fig. 6. 2 DOF robot arm

The dynamics of this robot arm is like as

$$\ddot{\theta}_1 = \{I'_3 I'_2 (\sin \theta_2) \dot{\theta}_2 (2\dot{\theta}_1 + \dot{\theta}_2) + I'_2 \bar{u}_1 - (I'_2 + I'_3 (\cos \theta_2)) \bar{u}_2\} / (I'_2 I'_1 - (I'_3)^2 (\cos \theta_2))$$

$$\ddot{\theta}_2 = \{-I'_3 (I'_2 + I'_3 (\cos \theta_2)) (\sin \theta_2) \dot{\theta}_2 (2\dot{\theta}_1 + \dot{\theta}_2) - (I'_2 + I'_3 (\cos \theta_2)) \bar{u}_1 + (I'_1 + I'_2 + 2I'_3 (\cos \theta_2)) \bar{u}_2\} / (I'_2 I'_1 - (I'_3)^2 (\cos \theta_2)^2)$$

where

The inertias of each link are  $I'_1 = 1.642 \text{Kg} \cdot \text{m}^2$ ,  $I'_2 = 0.382 \text{Kg} \cdot \text{m}^2$  and  $I'_3 = 0.138 \text{Kg} \cdot \text{m}^2$ . And both length of links are 0.35m.

And the parameters of SMCSPO is chosen as

$$\frac{k_{1j}}{\varepsilon_{oj}} = 3\lambda_d = 1050 \text{rad/s}$$

$$\frac{k_{2j}}{k_{1j}} = \lambda_d = 350 \text{rad/s},$$

$$\alpha_{3j} = \sqrt{\frac{\lambda_d}{3}} = \sqrt{350/3} \text{rad/s}$$

$$c_{j1} = K_j / \varepsilon_{oj} = \lambda_d = 350 \text{rad/s}$$

Fig. 7 shows that the position tracking errors are converged within about 0.35 mm. The performance of SMCSPO is superior to SMC. The comparison results of position tracking control of SMCSPO and SMC are shown in Fig. 8. Fig. 8 shows that SMCSPO is superior to SMC.

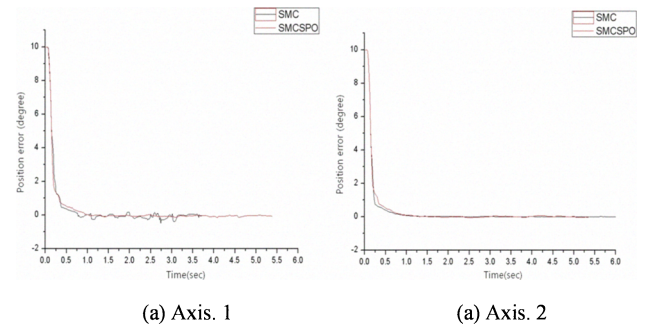


Fig. 7. Position error results

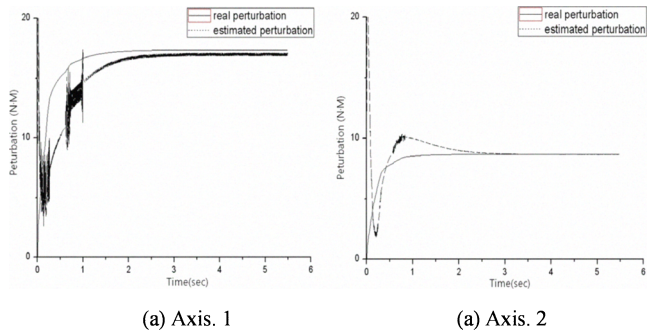


Fig. 8. Position tracking results

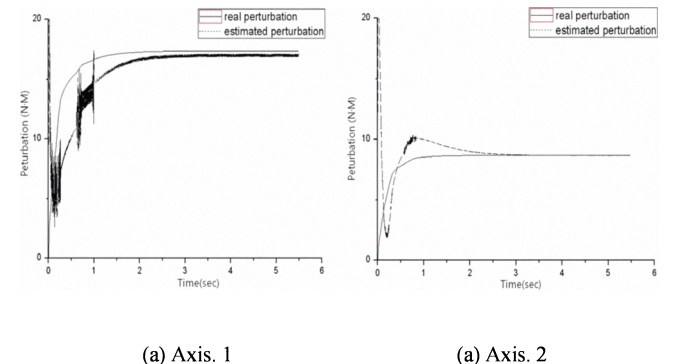


Fig. 9. Perturbation estimate results

## V. CONCLUSIONS

This paper designed the robust control algorithm for the surgical robot. The designed algorithm was applied to the 2 DOF robot arm for previous study of control of a surgical robot.

The designed control algorithm could reduce the inherent chattering as estimating the states and compensating a perturbation in accuracy. The designed observer was also proved to be superior to sliding observer due to the

perturbation estimation. The performance of SMCSPO is shown to be limited by the dominant time constant of the control process.

The results of simulation and experiment showed that SMCSPO can provide reliable tracking performance. The applied robust control algorithm has the merit that no additional sensor requires in the system.

So this is suitable for surgical robot which has difficulty to set up any sensor because of its structure.

#### REFERENCES

- [1] J. M. Sackier, Y. Wang, "Robotically assisted laparoscopic surgery: from concept to development," *Computer-Integrated Surgery*, R. Taylor, S. Lavallee, G. Burdea, and R. Mosges, Eds. Cambridge, MA: MIT Press, pp. 577-580, 1996
- [2] H. Hashimoto, K. Maruyama, and F. Harashima, "A Microprocessor-Based Robot Manipulator Control with Sliding Mode," *IEEE Trans. Industrial Electronics*, vol. 34, No. 1, pp. 11-18, 1987
- [3] J. J. Slotine, J. K. Hedrick, and E. A. Misawa, "On Sliding Observers for Non-Linear Systems," *ASME Journal of Dynamic Systems, Measurement and Control*, Vol. 109, pp. 245-252, 1987
- [4] H. Elmali and N. Olgac, "Sliding Mode Control with Perturbation Estimation (SMCPE)" *International Journal of Control*, Vol. 56, pp. 923-941, 1993
- [5] M. J. Terra, H. Elmali, and N. Olgac, "Sliding Mode Control With Sliding Perturbation Observer," *Journal of Dynamic Systems, Measurement, and Control*, Vol. 119, pp. 657-665, 1997
- [6] K. S. You, M. C. Lee and W. S. You "Sliding Mode Controller with Sliding Perturbation Observer Based on Gain Optimization using Genetic Algorithm," *KSME Int. J.*, vol. 18, No. 4, pp. 630-639, 2004
- [7] M. C. Lee, K. Son, and J. M. Lee, "Improving Tracking Performance of Industrial SCARA Robots Using a New Sliding Mode Control Algorithm," *KSME Int. J.*, vol. 12, No. 5, pp. 761-772, 1998
- [8] M. C. Lee and N. Aoshima, "Real Time Multi-Input Sliding Mode Control of a Robot Manipulator Based on DSP," *Proc. of SICE*, pp. 1223-1228, 1993